International Journal of Engineering Innovation & Research
Volume 9, Issue 1, ISSN: 2277 – 5668

Overview of Angle Estimation Algorithms in Bistatic MIMO Radar Systems

David Ebregbe
Department of Electrical and Electronic Engineering, Niger Delta University. Wilberforce Island Bayelsa State, Nigeria.
Corresponding author email id: ebregbed@gmail.com

Date of publication (dd/mm/yyyy): 25/02/2020

Abstract **– This paper gives an overview of the popular Subspace based Direction of Arrival (DOA) estimation techniques. Modern DOA estimation algorithms are based on subspace techniques. Subspace methods operate on a reduced parameter space by Eigen decomposition of the observed signal covariance matrix into two orthogonal spaces, the signal and noise subspaces and estimates the angles from one of these spaces. Subspace based DOA estimation techniques include; Multiple Signal Classification (MUSIC), Estimation of Signal Parameters via Rotational Invariance Technique (ESPRIT) and Unitary ESPRIT. These algorithms were originally formulated for single arrays. This paper extends their application to a bistatic MIMO (Multiple Input Multiple Output) radar system that have both a transmitting and a receiving array that are far apart. Performance comparison is made between the subspace based MUSIC algorithm and the spectral search based capon beam former using Matlab simulations. Several other Matlab simulations were run to demonstrate the application of ESPRIT and UNITARY ESPRIT algorithms on a bistatic MIMO System to estimate the Direction of Departure (DOD) and the Direction of Arrival (DOA) angles, the results showed how reduction in parameter space using subspace techniques reduces computational complexity and improves angle estimation resolution and accuracy.**

Keywords **– Bistatic MIMO Radar, Direction of Arrival, ESPRIT Algorithm, MUSIC Algorithm, Covariance Matrix.**

I. INTRODUCTION

Direction of arrival estimation of propagating signals constitutes a critical part of a wide range of engineering applications such as radar, sonar, environmental monitoring, public security, search and rescue, medical diagnosis, wireless communication, seismology and geophysics. Useful information carried by the propagating waves are retrieved through sensor arrays. A wide variety of Direction of arrival estimation algorithms that cuts across these application areas include Maximum likelihood techniques, the capon beam former and the subspace algorithms: Estimation of Signal Parameters via Rotational Invariance Technique (ESPRIT) and Multiple Signal Classification (MUSIC).

In array signal processing, an array of sensors, spatially distributed with respect to a reference sensor, spatially samples the amplitude and phase modified transmitted signals arriving at the array aperture. The output of the sensors consists of the desired signals corrupted by additive noise such as thermal noise as well as unwanted signals within the environment of the array aperture. Due to propagation delay, the signal at the output of each sensor element becomes a time advanced or time delayed version of the signal at the reference element [1]. Direction of arrival, which is one of the parameters that can be extracted from the received signals, is estimated from the delays between the elements of the array. The more spatial samples, that is, the number of elements in the array, the better the angle estimation resolution and detection capabilities.

There are several methods to Angle estimation. Some of the methods perform well in array geometries such as uniform linear arrays (ULAs), uniform circular arrays (UCAs) and uniform rectangular arrays (URAs). One of the earliest techniques of angle estimation is beamforming. Spectral estimation techniques like the capon method

were also used, but these techniques cannot estimate angles for closely spaced arrival angles for low signal-to-noise ratios (SNRs). Maximum Likelihood (ML) methods have been shown to have better performance among earlier classic angle estimation methods applicable to arbitrary geometries [2]. But this method has no closed form solution but instead it is iterative and a computationally demanding search is required.

Recent research activity on angle estimation has focused on the use of subspace techniques for their ability to reduce the parameter space and correspondingly the computational complexity. Subspace methods operate on a reduced parameter space by eigen decomposition of the observed signal covariance matrix into two orthogonal spaces, the signal and noise subspaces and estimates the angles from one of these spaces. In bistatic MIMO, the arrays are spaced far away from each other and the Direction-of-Departure (DOD) and Direction-of-Arrival (DOA) are different. Spatial synchronization in angle becomes a problem. In conventional bistatic radar, DOD/DOA synchronization is achieved by the transmitting beam and the receiving beam illuminating the target simultaneously. In [3] the subspace based ESPRIT algorithm is applied to bistatic MIMO radar by exploiting the dual invariance property of the transmitting and receiving arrays. This produces two rotational matrices whose eigenvalues correspond to the DODs and DOAs. But an additional pairing algorithm to match the DODs to the DOAs is required. For uniformly spaced antennas, Bencheikh et al [4] developed a combination of esprit and root MUSIC formulation to achieve automatic pairing of the angles and also avoids an exhaustive 2D MUSIC search to determine the DODs and DOAs. Target localization for bistatic MIMO based on subspace techniques is studied in [5], [6], [7], [8], [9]. Based on Lee's pioneering work on centro-hermitian matrices in converting a complex matrix to a real matrix using a Unitary transform [10]. Hardt and Nossek [11], and in reference [12] this transform is applied to the ESPRIT algorithm to develop the Unitary ESPRIT algorithm and its variants for multidimensional arrays. In [13], the Unitary ESPRIT algorithm is applied to the bistatic MIMO radar system exploiting the dual invariance and centrosymmetry of the bistatic MIMO radar system to provide real valued computations and automatically paired Directions of Departures (DOD) and Directions of Arrival (DOA) estimates. In all these studies, reduction in algorithm complexity and pairing has been achieved in different ways.

The rest of the paper is organized as follows: The classical approach to Angle estimation is presented in section II; in section III, we apply the classical angle estimation algorithms to a bistatic MIMO radar system; The Cramer Rao Bound for a bistatic MIMO is derived in section IV. Several Numerical examples based on Monte Carlo Simulations are presented and discussed in section V; and finally some conclusions are made in section VI.

Notation: $(\cdot)^H$, $(\cdot)^T$, $(\cdot)^*$, $(\cdot)^{-1}$ denote Hemitian transpose, transpose, complex conjugation without transposition and inverse respectively. diag(·) denotes the diagonalization operation. Vec(·) denotes a matrix operation that stacks the columns of a matrix under each other to form a new vector. We make use of the matlab expression $\mathbf{A}(m,n)$ to denote the elements of a $(M \times N)$ matrix **A.** $\otimes$ denotes the kronecker product.

II. Signal Model for a Bistatic MIMO Radar System

Consider a narrowband bistatic MIMO radar system consisting of M and N half - wavelength spaced omnidirectional antennas for the transmitting and receiving arrays respectively as shown in Fig 1. Assume both arrays are uniform linear arrays (ULA) and for sake of simplicity and clarity, we use a simple model with P uncorrelated targets with different doppler frequencies in the same range bin. All targets are in the far field of the transmitting and receiving arrays. Consider also that the target Radar Cross Section (RCS) is constant during a pulse period but fluctuates from pulse to pulse. This target model is a classical swerling case II model. The

directions of the p^{th} target with respect to the transmit array normal and receive array normal are denoted by θ_p (DOD) and ϕ_p (DOA) respectively. The transmitted waveforms are M orthogonal signals with identical bandwidth and centre frequency.

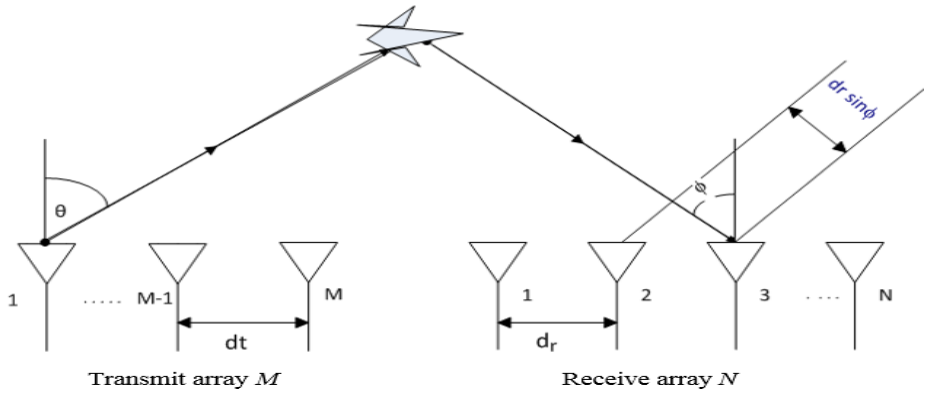

Fig. 1. Bistatic MIMO Configuration.

The coded signal of the m^{th} transmit antenna within one repetition interval is denoted by $\boldsymbol{s}_m \in C^{1\times L}$. Where, L denotes the length of the coding sequence within one repetition interval. For a radar system that uses K periodic pulse trains to temporally sample the signal environment, the received signals of the k^{th} pulse at the receiver array through reflections of the P targets can be written as [14], [15], [16],

$$\boldsymbol{X}_k = \sum_{p=1}^{P} \boldsymbol{a}_r\left(\phi_p\right)\beta_p \boldsymbol{a}_t^T\left(\theta_p\right)\begin{bmatrix}\boldsymbol{s}_1\\ \vdots \\ \boldsymbol{s}_M\end{bmatrix} e^{j\,2\,\pi\, f_{dp}\, t_k} + \boldsymbol{W}_k \tag{1}$$

Where, β_p denotes the RCS of the p^{th} target and f_{dp} denotes the Doppler frequency of the p^{th} target. $\boldsymbol{a}_r\,(\emptyset_p) = \left[1, e^{jr_p}, e^{j2r_p} \ldots\ldots e^{j(N-1)r_p}\right]^T$ and $\boldsymbol{a}_t\,(\theta_p) = \left[1, e^{ju_p}, e^{j2u_p} \ldots\ldots e^{j(M-1)u_p}\right]^T$ are the receive and transmit steering vectors respectively, $r_p = \pi \sin\phi_p$ and $u_p = \pi \sin\theta_p$. t_k denotes the slow time, k the slow time index and K the number of pulses or repetition intervals. Using the orthogonality property of the transmitted waveforms, ($\boldsymbol{s}_i \boldsymbol{s}_j = 0$ and $\|\boldsymbol{s}_i\|^2 = 1,\ i \neq j = 1.....M$), the output of the matched filters with the m^{th} transmitted baseband signal can be expressed as

$$\boldsymbol{Y}_m\left(t_k\right) = \sum_{p=1}^{P} \boldsymbol{a}_r\left(\phi_p\right)\beta_p \boldsymbol{a}_t^T\left(\theta_p\right)\begin{bmatrix}0\\ \vdots \\ \mathbf{s}_m \\ \vdots \\ 0\end{bmatrix} e^{j2\pi f_{d\,p} t_k} + \boldsymbol{V}_m\left(t_k\right) \tag{2}$$

The data matrix in Equation (2) is usually vectorized by stacking the columns of $\boldsymbol{Y}_m(t_k)$. Let $\mathbf{z}(t_k) \in C^{MN\times 1}$ be the output of all the received signal.

$$\mathbf{z}(t_k) = \left[\boldsymbol{Y}_1^T(t_k), ..., \boldsymbol{Y}_M^T(t_k)\right]^T \tag{3}$$

$$\mathbf{z}(t_k) = \boldsymbol{A}\boldsymbol{s}(t_k) + \boldsymbol{n}(t_k) \tag{4}$$

Where $\mathbf{A}=\left[\mathbf{a}_r(\phi_1)\otimes\mathbf{a}_t(\theta_1),.....,\mathbf{a}_r(\phi_p)\otimes\mathbf{a}_t(\theta_p)\right]$ is the $MN\times P$ steering matrix. $\mathbf{n}(t_k)=\text{vec}(\mathbf{V}_m(t_k))$ is the additive white Gaussian noise of zero mean and covariance, $\sigma^2\mathbf{I}_{MN}$ after match filtering and $\boldsymbol{I}_{MN}$ is a $MN\times MN$ identity matrix. $\mathbf{s}(t_k)=r(t_k)\left[\beta_1\, e^{j2\pi f_{d1}t_k}\, e^{j\varphi_1}\ldots\ldots\beta_P e^{j2\pi f_{dP}t_k}\, e^{j\varphi_P}\right]^T$. The covariance matrix for K snapshots of $\mathbf{z}(t)$ is estimated by $\mathbf{R}_z=\frac{1}{K}\sum_{t=1}^{K}\mathbf{z}(t)\,\mathbf{z}^H(t)$, where $(\cdot)^H$ represents the Hermitian transpose.

$$\mathbf{R}_z=\mathbf{E}_s\boldsymbol{\Lambda}_s\mathbf{E}_s^H+\mathbf{E}_{no}\boldsymbol{\Lambda}_{no}\mathbf{E}_{no}^H \tag{5}$$

A. *2D-MUSIC and 2D-Capon*

We formulate the 2D-MUSIC and 2D-Capon spatial spectrum functions [17], [18], [19], 20] as

$$P_{music}(\theta,\phi)=\frac{1}{\left[\mathbf{a_r}(\phi)\otimes\mathbf{a_t}(\theta)\right]^H\mathbf{E_{no}}\mathbf{E}_{no}^H\left[\mathbf{a_r}(\phi)\otimes\mathbf{a_t}(\theta)\right]} \tag{6}$$

$$P_{capon}(\theta,\phi)=\frac{1}{\left[\mathbf{a_r}(\phi)\otimes\mathbf{a_t}(\theta)\right]^H\mathbf{R_z}^{-1}\left[\mathbf{a_r}(\phi)\otimes\mathbf{a_t}(\theta)\right]} \tag{7}$$

$\mathbf{E_{no}}$ is the noise subspace involving the eigenvectors corresponding to the last $MN–P$ eigenvalues by eigen decomposition of $\mathbf{R_z}$. The DODs and DOAs of the targets can be obtained by a two-dimensional search, which is computationally very intensive.

B. *Unitary ESPRIT for Bistatic MIMO Radar*

In this part, we apply an angle estimation algorithm for a bistatic MIMO radar system based on Unitary ESPRIT techniques. This algorithm exploits the dual invariance in distinct directions and centrosymmetry of the bistatic MIMO radar system to provide real valued computations and automatically paired Directions of Departures (DOD) and Directions of Arrival (DOA) [13].

The dual invariance property of the transmitting and receiving arrays is exploited to produce two rotational matrices whose eigenvalues correspond to the DODs and DOAs.

Let $T_p=e^{ju_p}$ and $R_p=e^{jr_p}$, then $\mathbf{a}_t(\theta_p)=\left[1,T_p,T_p^2\ldots\ldots T_p^{M-1}\right]^T$ and $\mathbf{a}_r(\phi_p)=\left[1,R_p,R_p^2\ldots\ldots R_p^{N-1}\right]^T$.

Each column of the matrix, $\boldsymbol{A}$ in equation (4) corresponds to a MN element virtual array for the p^{th} target.

$$\mathbf{A}(:,p)=\mathbf{a}_r(\phi_p)\otimes\mathbf{a}_t(\theta_p) \tag{8}$$

$$=[1,T_p,\ldots,T_p^{M-1},R_p,R_pT_p,\ldots,R_pT_p^{M-1},\ldots,R_p^{N-1},R_p^{N-1}T_p,\ldots,R_p^{N-1}T_p^{M-1}]^T$$

Exploring, the structure of this MN element virtual array manifold, the two pairs of selection matrices for both the transmitting and receiving arrays must be chosen to be centrosymmetric with respect to one another. The maximum overlap subarrays consisting of the first and last M-1 elements of the transmit array steering vectors, $\mathbf{a}_t(\theta_p)$ in the complete MN virtual array occurs N times. The selection matrices are $\mathbf{J}_1$ and $\mathbf{J}_2$ both M-1xM-1 matrices occurring N times

$$\mathbf{J}_1=\mathbf{I}_{N\times N}\otimes\left[\mathbf{I}_{(M-1)\times(M-1)}\quad\mathbf{0}_{(M-1)\times1}\right] \tag{9}$$

$$\mathbf{J}_2 = \mathbf{I}_{N\times N} \otimes \left[\mathbf{0}_{(M-1)\times 1} \quad \mathbf{I}_{(M-1)\times(M-1)}\right] \tag{10}$$

The shift invariance property for the transmit array from the columns of $\boldsymbol{A}$ can be expressed as

$$\mathbf{J}_1\mathbf{A} = \mathbf{J}_2\mathbf{A}\boldsymbol{\Phi}_t \tag{11}$$

Where $\boldsymbol{\Phi}_t = diag\left\{e^{ju_p}\right\}_{p=1}^{P}$. For incoherent signal sources, the columns of $\mathbf{E_s}$ and $\mathbf{A}$ span the same subspace. Therefore, using equations (9) to (10),

$$\boldsymbol{\Psi}_t = \mathbf{T}^{-1}\boldsymbol{\Phi}_t\mathbf{T} \tag{12}$$

The DODs are estimated from the eigenvalues of $\boldsymbol{\Psi}_t$. Again, looking at the *MN* element virtual array manifold of equation (50), the elements of the receive array steering vectors, $\mathbf{a}_r(\phi_p)$ are distributed across the *MN* virtual array in such a way that each element occurs *M* times in the *MN* virtual array. Therefore the maximum overlap subarrays of the receive steering vectors consists of the first and last *M*(*N*-1) of the *MN* virtual array elements. The selection matrices for the receive array are as follows;

$$\mathbf{J}_3 = \left[\mathbf{I}_{M(N-1)\times M(N-1)} \quad \mathbf{0}_{M(N-1)\times M}\right] \tag{13}$$

$$\mathbf{J}_4 = \left[\mathbf{0}_{M(N-1)\times M} \quad \mathbf{I}_{M(N-1)\times M(N-1)}\right] \tag{14}$$

And the shift invariance equations for the receive array, from which the DOAs can be obtained is expressed as

$$\mathbf{J}_3\mathbf{A} = \mathbf{J}_4\mathbf{A}\boldsymbol{\Phi}_r \tag{15}$$

Where $\boldsymbol{\Phi}_r = diag\left\{e^{jr_p}\right\}_{p=1}^{P}$. Using the same procedure for determining the DODs, The DOAs are determined from the eigenvalues of

$$\boldsymbol{\Psi}_r = \mathbf{T}^{-1}\boldsymbol{\Phi}_r\mathbf{T} \tag{16}$$

We then use a unitary transform to map the complex valued virtual array manifold to a real valued one. The 2*F* and 2*F*+1 unitary matrices are expressed as

$$\boldsymbol{Q}_{2F} = \frac{1}{\sqrt{2}}\begin{bmatrix} \boldsymbol{I}_F & j\boldsymbol{I}_F \\ \boldsymbol{\Pi}_F & -j\boldsymbol{\Pi}_F \end{bmatrix} \quad \text{for even } F \tag{17}$$

$$\boldsymbol{Q}_{2F+1} = \frac{1}{\sqrt{2}}\begin{bmatrix} \boldsymbol{I}_F & \mathbf{0} & j\boldsymbol{I}_F \\ \mathbf{0}^T & \sqrt{2} & \mathbf{0}^T \\ \boldsymbol{\Pi}_F & \mathbf{0} & -j\boldsymbol{\Pi}_F \end{bmatrix} \quad \text{for odd } F \tag{18}$$

Where, $\boldsymbol{\Pi}_F$ denotes an *F* x *F* exchange matrix with ones on its antidiagonal and zeros elsewhere.

The Unitary transformed virtual array steering matrix is obtained as $\boldsymbol{G} = \boldsymbol{Q}_{MN}^{H}\boldsymbol{A}$. Similar shift invariance equations as in (11) and (15) can be derived for the real valued virtual array manifold **G** using the same selection matrices as derived in equations (9) and (10) for the transmit array and equations (13) and (14) for the receive array. The transformed selection matrices and invariance equations are obtained a

$$\boldsymbol{K}_1 = \mathrm{Re}\left\{(\boldsymbol{Q}^H_{(M-1)N}\, \boldsymbol{J}_2\, \boldsymbol{Q}_{MN})\right\} \; and \; \boldsymbol{K}_2 = \mathrm{Im}\left\{(\boldsymbol{Q}^H_{(M-1)N}\, \boldsymbol{J}_2\, \boldsymbol{Q}_{MN})\right\} \tag{19}$$

$$\boldsymbol{K}_1 \boldsymbol{G} \boldsymbol{\Omega}_t = \boldsymbol{K}_2 \boldsymbol{G} \tag{20}$$

$$\boldsymbol{K}_3 = \mathrm{Re}\left\{(\boldsymbol{Q}^H_{M(N-1)}\, \boldsymbol{J}_4\, \boldsymbol{Q}_{MN})\right\} \; and \; \boldsymbol{K}_4 = \mathrm{Im}\left\{(\boldsymbol{Q}^H_{M(N-1)}\, \boldsymbol{J}_4\, \boldsymbol{Q}_{MN})\right\} \tag{21}$$

$$\boldsymbol{K}_3 \boldsymbol{G} \boldsymbol{\Omega}_r = \boldsymbol{K}_4 \boldsymbol{G} \tag{22}$$

Where $\boldsymbol{\Omega}_t = diag\left\{\tan\left(t_p/2\right)\right\}_{p=1}^{P}$ and $\boldsymbol{\Omega}_r = diag\left\{\tan\left(r_p/2\right)\right\}_{p=1}^{P}$. The $MN \times P$ real valued matrix of signal eigenvectors $\boldsymbol{E}_s$ spans the same P dimensional subspace as the $MN \times P$ real valued steering matrix $\boldsymbol{G}$. Therefore there exists a nonsingular matrix $\boldsymbol{H}$ of size $P \times P$ such that $\boldsymbol{E}_s = \boldsymbol{G}\boldsymbol{H}$.

Substituting this in Equations (20) and (22) yields the transformed invariance equations which can be used to compute the DODs. And DOAs.

$$\boldsymbol{K}_1 \boldsymbol{E}_s \boldsymbol{\Psi}_t = \boldsymbol{K}_2 \boldsymbol{E}_s \tag{23}$$

$$\boldsymbol{K}_3 \boldsymbol{E}_s \boldsymbol{\Psi}_r = \boldsymbol{K}_4 \boldsymbol{E}_s \tag{24}$$

Where $\boldsymbol{\Psi}_t = \boldsymbol{H}\boldsymbol{\Omega}_t\boldsymbol{H}^{-1}$ and $\boldsymbol{\Psi}_r = \boldsymbol{H}\boldsymbol{\Omega}_r\boldsymbol{H}^{-1}$. Since both $\boldsymbol{\Psi}_t$ and $\boldsymbol{\Psi}_r$ share the same transform matrix $\boldsymbol{H}$ and are also real valued matrices, automatically paired estimates of DODs and DOAs $\left\{t_p, r_p\right\}, p = 1\cdots\cdots$ can be obtained from the real and imaginary parts of the eigenvalues obtained by the eigen decomposition of the complex valued matrix

$$\boldsymbol{\Psi}_t + j\boldsymbol{\Psi}_r = \boldsymbol{H}\left(\boldsymbol{\Omega}_t + j\boldsymbol{\Omega}_r\right)\boldsymbol{H}^{-1} \tag{25}$$

Where $\boldsymbol{\Omega}_t + j\boldsymbol{\Omega}_r = diag\left\{\lambda_p\right\}_{p=1}^{P}$, are the eigenvalues. The DODs and DOAs are obtained as

$$\hat{\theta}_p = \arcsin\left\{2\arctan\left(\mathrm{Re}\left\{\lambda_p\right\}\right)\right\} \tag{26}$$

$$\hat{\phi}_p = \arcsin\left\{2\arctan\left(\mathrm{Im}\left\{\lambda_p\right\}\right)\right\} \quad p = 1\ldots\ldots \tag{27}$$

III. Cramer Rao Bound

The accuracy of angle estimation is very important. The Cramer Rao bound provides the lower limit on the Mean-Square-Error (MSE) that can be achieved by any unbiased estimator. The first step in the derivation of the CRB is determining the elements of the Fisher Information Matrix (FIM). The FIM for a Multivariate normal distribution of mean, $\mu = 0$ and Covariance, R_z i.e $N^c(\mu(\theta)R_z(\theta))$ has elements represented as

$$\mathbf{J}_{m,n} = \frac{\partial \boldsymbol{\mu}^T}{\partial \theta_m}\mathbf{R}_z^{-1}\frac{\partial \boldsymbol{\mu}}{\partial \theta_n} + \frac{1}{2}\mathrm{tr}\left(\mathbf{R}_z^{-1}\frac{\partial \mathbf{R}_z}{\partial \theta_m}\mathbf{R}_z^{-1}\frac{\partial \mathbf{R}_z}{\partial \theta_n}\right) \tag{28}$$

Where $(.)^T$ denotes transpose and tr(.) denotes the trace of a square matrix. The signal model (4) is a multivariate normal distribution of zero mean and covariance $\mathbf{R}_z$ where $\mathbf{R}_z = E\left\{\mathbf{z}\mathbf{z}^H\right\} \approx (1/K)\mathbf{z}\mathbf{z}^H$ is a MN x MN data covariance

matrix [17].

$$\mathbf{J}(\boldsymbol{\eta}) = \frac{1}{2}\mathrm{tr}\left(\mathbf{R}_z^{-1}(\boldsymbol{\eta})\frac{\partial \mathbf{R}_z(\boldsymbol{\eta})}{\partial \boldsymbol{\eta}}\mathbf{R}_z^{-1}(\boldsymbol{\eta})\frac{\partial \mathbf{R}_z(\boldsymbol{\eta})}{\partial \boldsymbol{\eta}}\right) = \begin{bmatrix} \mathbf{J}_{\theta\theta} & \mathbf{J}_{\theta\phi} & \mathbf{J}_{\theta\beta} & \mathbf{J}_{\theta\sigma} \\ \mathbf{J}_{\theta\phi}^T & \mathbf{J}_{\phi\phi} & \mathbf{J}_{\phi\beta} & \mathbf{J}_{\phi\sigma} \\ \mathbf{J}_{\theta\beta}^T & \mathbf{J}_{\phi\beta}^T & \mathbf{J}_{\beta\beta} & \mathbf{J}_{\beta\sigma} \\ \mathbf{J}_{\theta\sigma}^T & \mathbf{J}_{\phi\sigma}^T & \mathbf{J}_{\beta\sigma}^T & \mathbf{J}_{\sigma\sigma} \end{bmatrix} \tag{29}$$

Where $\boldsymbol{\eta} = [\boldsymbol{\theta}\ \boldsymbol{\phi}\ \boldsymbol{\beta}\ \sigma]^T$, $\boldsymbol{\beta} = \left[\beta_{1,\ldots\ldots,\beta_p}\right]^T$, $\boldsymbol{\theta} = \left[\theta_{1,\ldots\ldots,\theta_p}\right]^T$ and $\boldsymbol{\theta} = \left[\theta_{1,\ldots\ldots,\theta_p}\right]^T$ the submatrices are derived in Appendix A of [24], The variance of individual estimated parameters can be obtained by inverting the FIM

$$\mathbf{CRB}(\boldsymbol{\eta}) = diag\left(\mathbf{J}^{-1}(\boldsymbol{\eta})\right) \tag{30}$$

The corresponding CRB for joint DOD and DOA for a single target for a bistatic MIMO is given as [21],

$$\boldsymbol{CRB}(\theta_1,\phi_1) = \frac{1}{2MNK\pi^2\sum_{k=1}^{K}\left|\beta(k)\right|^2/\left(K\sigma^2\right)}\begin{bmatrix} 6\Big/\left[\left(M^2-1\right)\cos^2\theta_1\right] & 0 \\ 0 & 6\Big/\left[\left(N^2-1\right)\cos^2\phi_1\right] \end{bmatrix} \tag{31}$$

IV. NUMERICAL SIMULATIONS

A. *Unitary Esprit and Standard Esprit for Bistatic MIMO*

In this part of the simulations, we evaluate the performance of the Unitary ESPRIT as proposed in [13]. First, consider a uniform linear array (ULA) of 3 antennas at the transmitter and 4 antennas at the receiver, both of which have a half wavelength spacing between its antennas. There are 8 targets with locations, RCSs and Doppler frequencies as shown in table 1. The pulse repetition frequency is 10 kHz. The operating frequency is 30GHz and the pulse width is 10μs. The SNR = 10dB. 256 snapshots of the received signal corrupted by a zero mean spatially white noise with variance of one were observed. For the purpose of statistical repeatability, 500 Monte Carlo trials with a SNR of 10dB were run.

Table 1. Target Parameters.

Targets	**1**	**2**	**3**	**4**	**5**	**6**	**7**	**8**
DOD(θ)	-20	-50	-10	-40	60	30	40	20
DOA(ϕ)	-40	-20	10	40	0	50	30	-25
β	1	1	1	1	1	1	1	1
f_d(Hz)	1000	1500	2000	2500	3000	3500	4000	4500

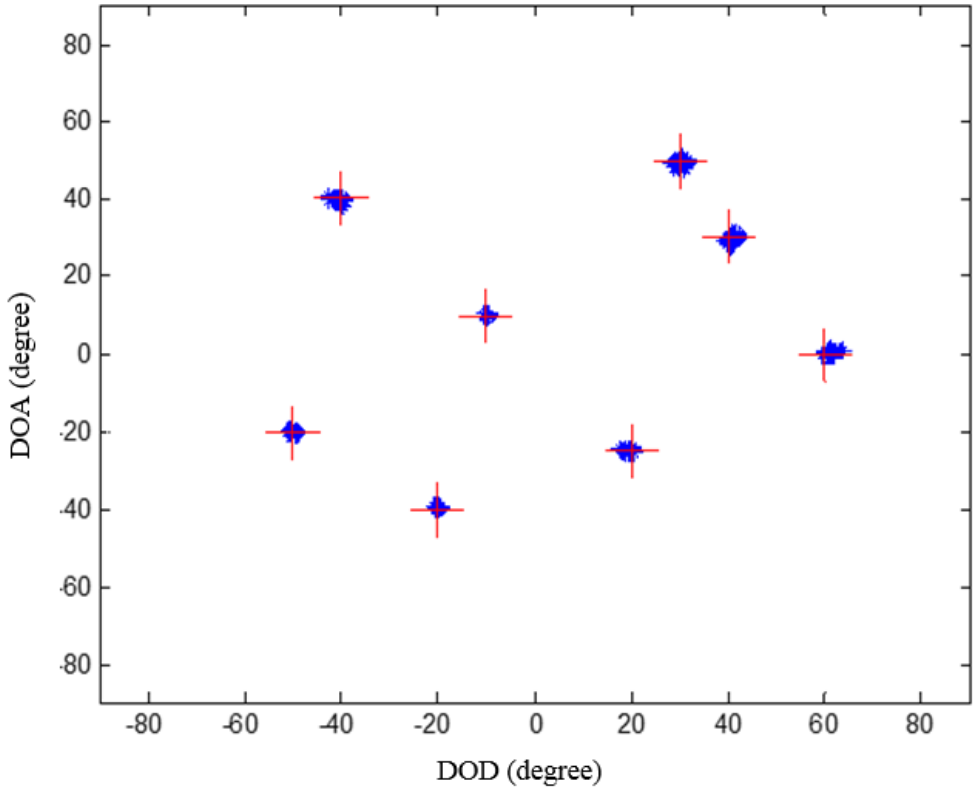

Fig. 3. Joint angle estimation for Unitary ESPRIT algorithm for 8 targets over 500 monte carlo trials.

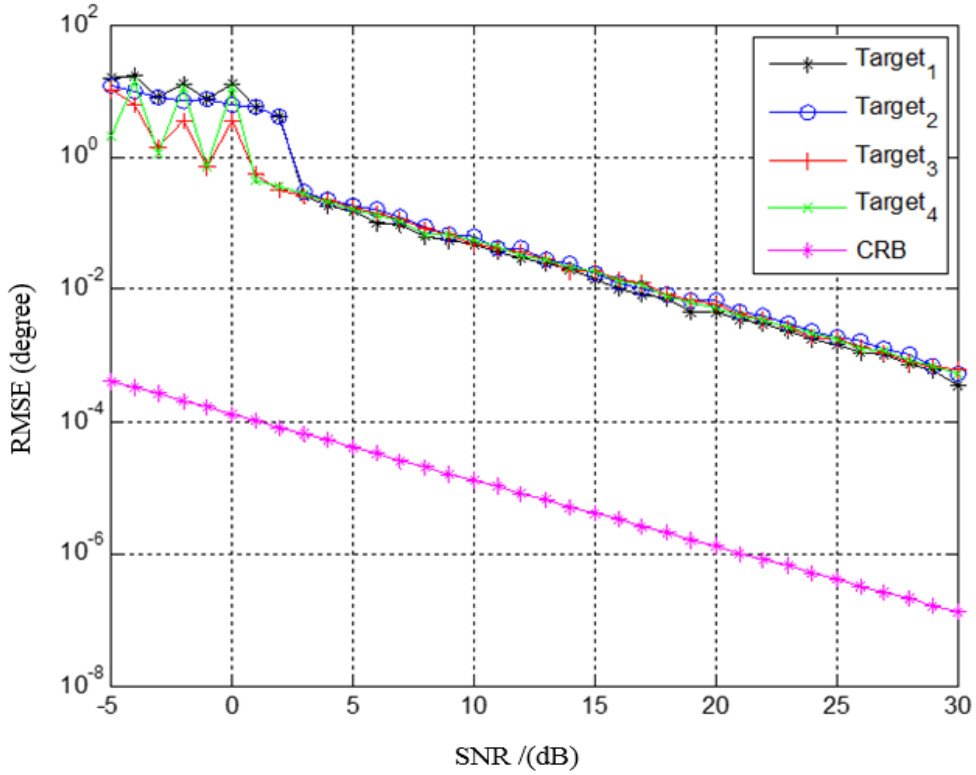

Fig. 4. RMSE of estimation of P = 4 targets versus SNR with M = 8, N = 6, K = 256 for 200 monte carlo trials.

Fig. 3 shows the targets are localized and paired correctly. Secondly, retaining the same number of antennas and spacing as the first simulation we evaluate the performance of the algorithm with 4 targets from angles (θ_1, ϕ_1) = (10°, 20°), (θ_2, ϕ_2) = (-8°, 30°), (θ_3, ϕ_3) = (0°, 45°) (θ_4, ϕ_4) = (50°, 60°) with reflection coefficients $\beta_1 = \beta_2 = \beta_3 =$

$\beta_4 = 1$ and Doppler frequencies $f_{d1} = 1000$Hz, $f_{d2} = 1500$ Hz, $f_{d3} = 2500$ Hz and $f_{d4} = 3000$ Hz. We use the Root Mean Square Error (RMSE) performance criterion. The RMSE of the p^{th} target angle estimation is defined as $\text{RMSE}_p = \sqrt{1/L \sum_{l=1}^{L} \left(\hat{\theta}_{pl} - \theta_p\right)^2 + \left(\hat{\phi}_{pl} - \phi_p\right)^2}$ where, L is the Monte Carlo trial number, $\hat{\theta}_{pl}$ and $\hat{\phi}_{pl}$ are the estimates at the l^{th} iteration, θ_p and ϕ_p are true values. The number of samples is K = 256 and SNRs were varied from -5 to 30dB. Results are obtained using 200 Monte Carlo simulations. Fig. 4 shows the RMSE versus SNR for the 4 targets. The estimation errors are quite negligible.

Thirdly, we compare the RMSE of target angle estimation of the Unitary ESPRIT algorithm to that of the conventional ESPRIT algorithm for a bistatic MIMO radar system. The parameters and simulation conditions are the same as the previous simulation. Fig. 5 shows a comparison of the RMSE of the Unitary ESPRIT algorithm versus RMSE for the Conventional ESPRIT at different SNRs for one target. The RMSEs for the other targets are similar. The Unitary ESPRIT algorithm yields excellent estimates with negligible errors and performs better for both low and high SNRs, compared to the conventional ESPRIT algorithm.

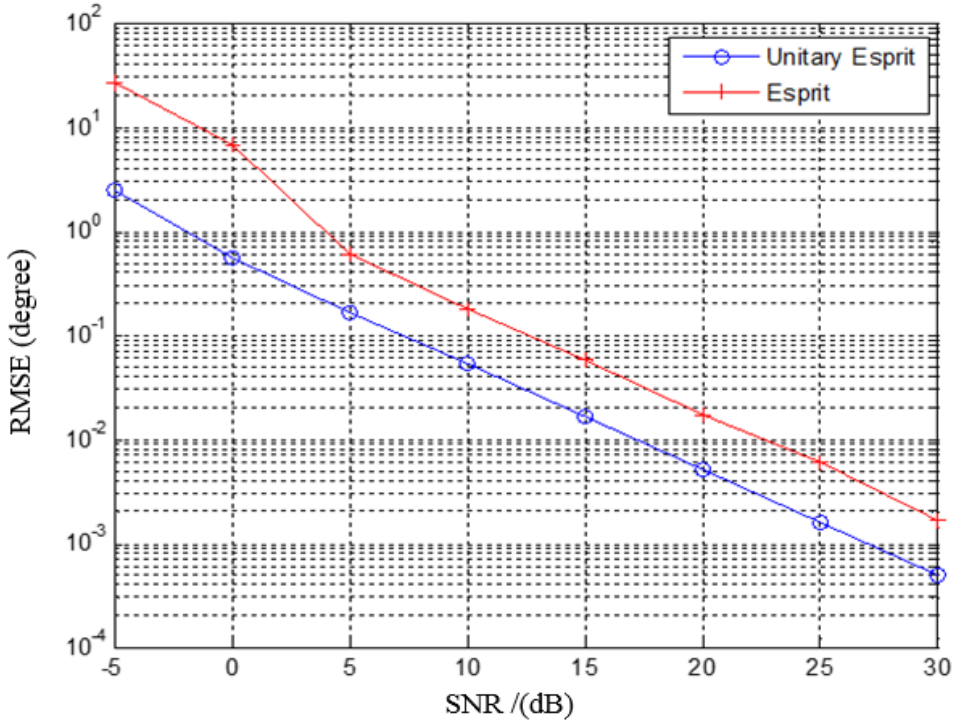

Fig. 5. RMSE of estimation versus SNR for M = 8, N = 6, and K = 256 samples for 200 monte carlo trials.

B. *2D Capon and 2D Music for Bistatic MIMO*

In this part of the simulations, we investigate and compare the performance of the search based 2D Capon and 2D MUSIC algorithms. The bistatic MIMO radar parameters and configurations are the same as the previous simulations in part A. Four targets are located at (DOD, DOA) = (-30^0, -40^0), (-50^0, -20^0), (10^0, 10^0), (-10^0, 30^0). The number of snapshots $K = 256$. 10 monte carlo trials were performed at SNRs of 10dB and 30dB. Fig. 6 and Fig. 7 show the 2D MUSIC spectrum and 2D capon spectrum at 10dB while Fig. 8 and Fig. 9 shows the spectrums at 30dB. With the MUSIC algorithm, a clear spatial spectrum can be seen with targets identified by peaks more clearly than the Capon algorithm at a low SNR of 10dB. However, as the number of antennas is decreased, the Capon algorithm is able to identify peaks more clearly than the MUSIC algorithm.

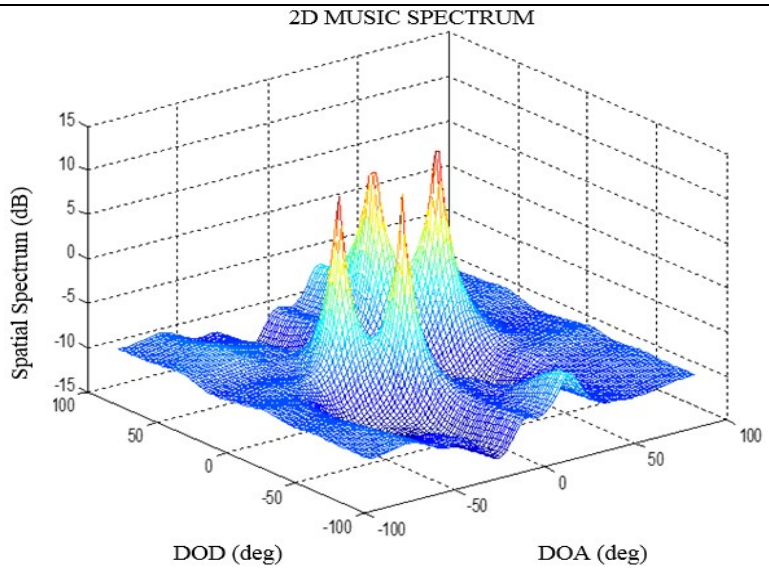

Fig. 6a. 2D MUSIC at 10dB.

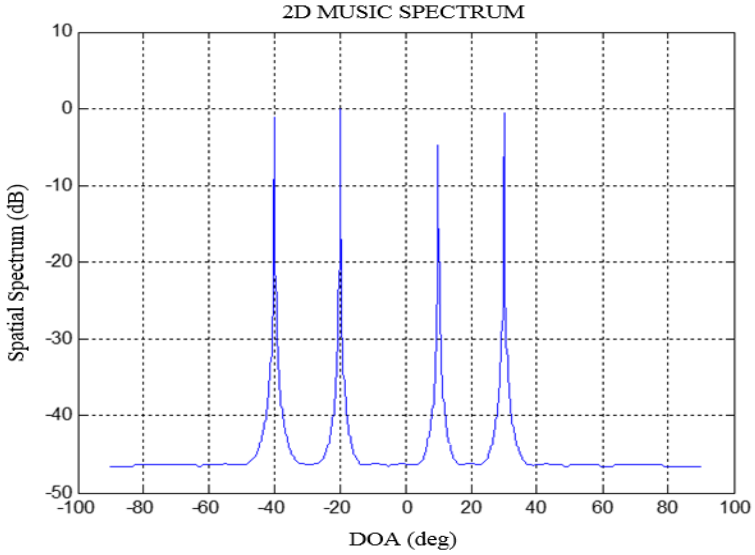

Fig. 6b. 2D MUSIC DOA at 10dB.

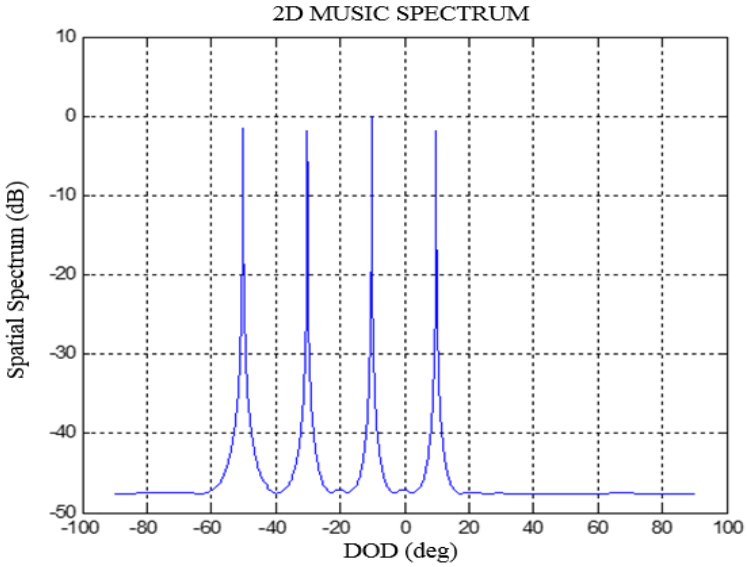

Fig. 6c. 2D MUSIC DOD at 10dB.

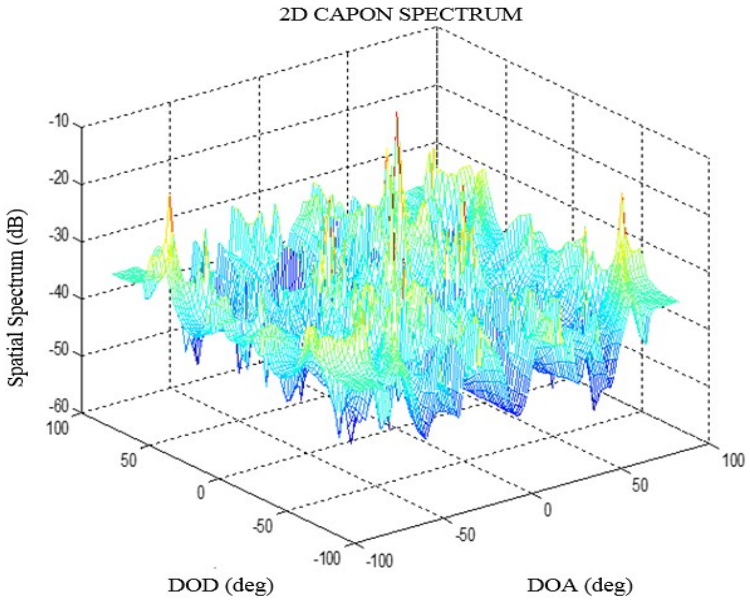

Fig. 7a. 2D Capon at 10dB.

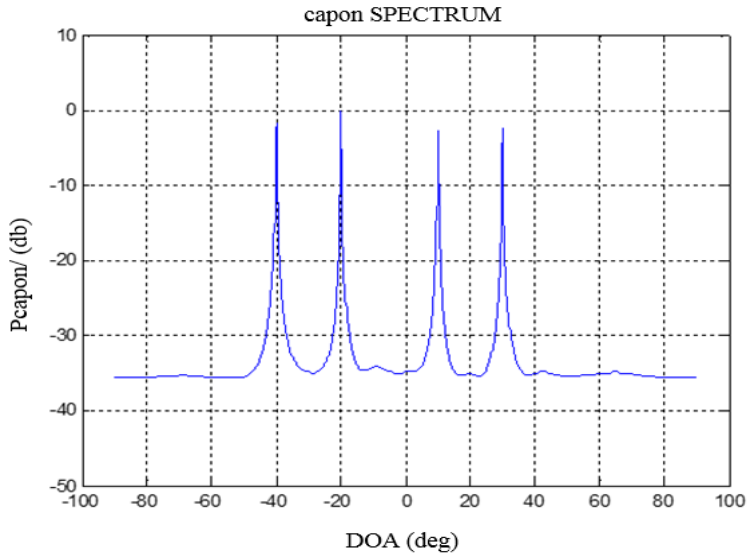

Fig. 7b. 2D Capon DOA at 10dB.

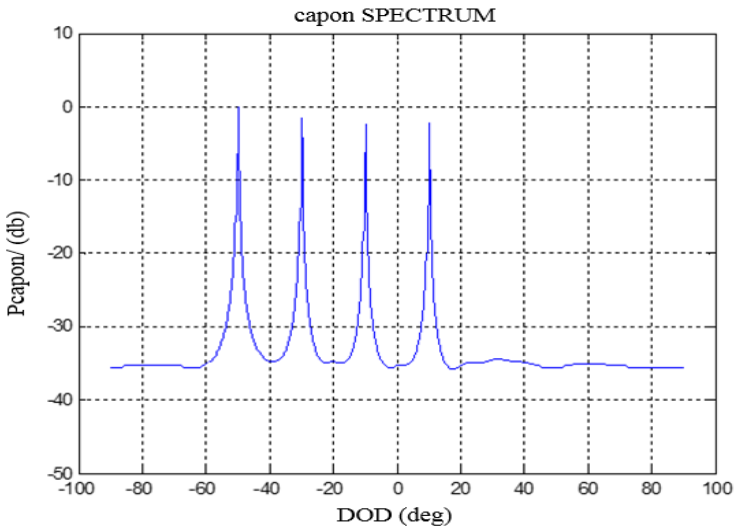

Fig. 7c. 2D Capon DOD at 10dB.

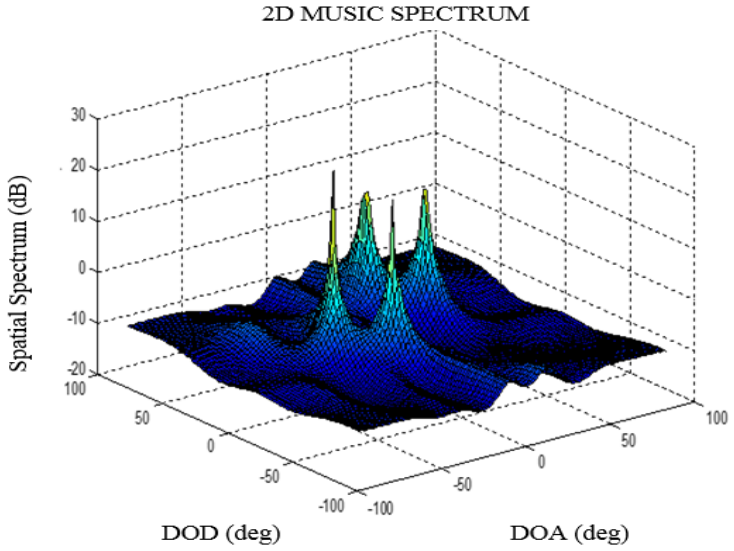

Fig. 8. 2D MUSIC Spectrum at 30dB.

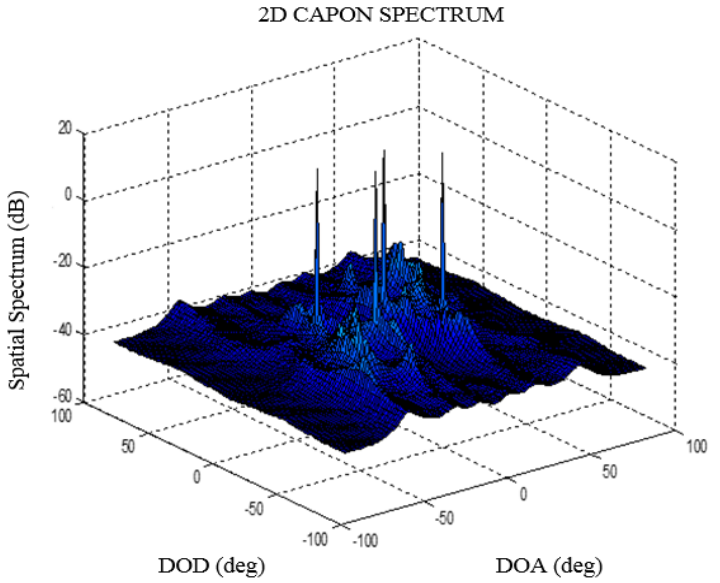

Fig. 9. 2D Capon at 30dB.

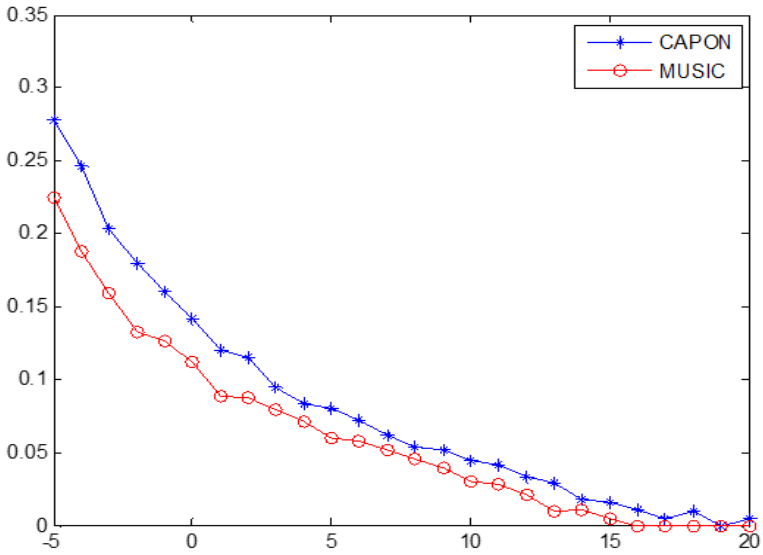

Fig. 10. RMSE of MUSIC versus Capon at different SNRs.

V. CONCLUSIONS

In this paper, various subspace algorithms were applied to a bistatic MIMO radar system to estimate target angles. Both MUSIC and Capon are search based algorithms and are therefore computationally more costly than the algebraic methods of ESPRIT and UNITARY ESPRIT. While Capon and ESPRIT work on the signal subspace, MUSIC works on the Noise subspace only based on the orthogonality of the steering vectors and the noise subspace eigenvectors. The MUSIC algorithm performs poorly for a reduced number of antennas both at the transmitting and receiving arrays for low SNRs due to its inability to truly separate the signal subspace from the noise subspace. At low SNRs the resolution of the Capon algorithm is very poor; while MUSIC returns clear target peaks at the same SNR. Furthermore MUSIC estimates are asymptotically more efficient than the capon estimates at different SNRs. The simulation results also show that the Unitary ESPRIT algorithm yields excellent estimates with negligible errors and performs better for both low and high SNRs, compared to the conventional ESPRIT algorithm. The number of targets that can be detected is increased and there is a lower computational complexity as the algorithm uses only real computations.

REFERENCES

[1] 1 Pillai S.U. Array Signal Processing, pp 3-15, Springer-Verlag, 1989.
[2] Gershman A.B, M. Rubsamen and M. Pesavento, One and two dimensional direction-of-arrival estimation: An overview of search free techniques, Elsevier Signal processing vol, 90 issue 5, pp 1338-1349, 2010.
[3] Duofang C, Baixiao C, Guodong Q, Angle estimation using ESPRIT in MIMO radar, IEEE Electronic. Letters. 44 (12) (5th June 2008
[4] Bencheikh M.L. and Wang Y. Joint DOD-DOA estimation using combined ESPRIT-MUSIC approach in MIMO radar. Electronics Letters 22nd July 2010 Vol. 46 No. 15.
[5] Jiang M., J. Huang, Y. Hou, ESPRIT Method for Multiple-Target Localization using MIMO Array, IEEE 9th Int. Conf. on Signal Processing, pp. 84-87, 2008.
[6] Jinli C., Hong, G., and Weimin, S. Angle estimation using ESPRIT without pairing in MIMO radar, Electron. Lett., 2008, 44, (24), pp. 1422–1423.
[7] Li C, Liao G, Zhu S and Wu S. An ESPRIT-like algorithm for coherent DOA estimation based on data matrix decomposition in MIMO radar. Signal Process. doi:10.1016/j.sigpro.2011.02.004.
[8] Liu F and Wang L. An Effective Virtual ESPRIT Algorithm for Multi-target Localization in Bistatic MIMO Radar System 2010 International Conference on Computer Design and Applications (ICCDA 2010), pp V4-412 - V4-415.
[9] Liu X. L and Liao G.S. Multi-target localization in bistatic MIMO radar Electronics Letters 24 th June 2010 Vol. 46 No.13, Pp 945-946.
[10] Lee A. "Centrohermitian and skew-centrohermitian matrices," *Linear Algebra and its Applications*, vol. 29, pp. 205–210, 1980.
[11] M. Haardt and J.A. Nossek, "Simultaneous Schur decomposition of several non- symmetric matrices to achieve automatic pairing in multidimensional harmonic retrieval problems," *IEEE Trans. Signal Processing*, vol. 46, pp. 161–169, Jan. 1998.
[12] Zoltowski, M.D., Haardt, M., and Mathews, C.P.: 'Closed-form 2-D angle estimation with rectangular arrays in element space or beamspace via unitary ESPRIT', IEEE Trans. Signal Process., 1996, 44, (2), pp. 316–328.
[13] Ebregbe D, D. Weibo and Y Songyan Angle Estimation in Bistatic MIMO Radar System based on Unitary ESPRIT. Research Journal of Applied Sciences, Engineering and Technology. Vols. 7 (2014), Issue 3. pp. 521-526.
[14] Bencheikh M.L., Wang, Y., and He, H, Polynomial root finding technique for joint DOA DOD estimation in bistatic MIMO radar, Signal Process., 90, (9), pp. 2723–2730.
[15] Chen J., Gu H and Su W. A new method for joint DOD and DOA estimation in bistatic MIMO radar. Signal Processing 90 (2010) 714–718.
[16] Jin M, Liao G, Li J, Joint DOD and DOA estimation for bistatic MIMO radar, Signal Processing 89 (2009) 244–251.
[17] Haidong Yan, Jun Li and Guisheng Liao, Multi target Identification and Localization using Bistatic MIMO Radar Systems, EURASIP Journal on Advances in Signal Processing, vol. 2008, Article ID 283483, 8 pages, 2008. doi:10.1155/2008/283483.
[18] Liu X, Liao G., Reduced-dimensional Angle Estimation in Bistatic MIMO Radar System. IEEE CIE Int. conf. on Radar, Vol. 1, pp 67-70, 2011.
[19] Zhang X and Xu D. Angle estimation in MIMO radar using reduced-dimension capon Electronics Letters 10th June 2010 Vol. 46 No.12.
[20] Zhao Y, P. Shui, H. Liu, Computationally Efficient DOA Estimation for MIMO Radar, IEEE 2nd Int. Conf. on Image and Signal Processing CISP pp 1-3, 2009
[21] Bencheikh M.L, Wang Y. Non Circular Esprit-Rootmusic Joint Doa-Dod Estimation in Bistatic MIMO Radar. 7th International Workshop on Systems, Signal Processing and their Applications (WOSSPA). 2011. Pp 51-54.
[22] Schmidt R.O. Multiple Emitter Location and Signal Parameter Estimation. IEEE Transactions on Antennas And Propagation, Vol. Ap-34, No. 3, March 1986.
[23] Swindlehurst A., B. Ottersten, R. Roy, and T. Kailath, Multiple Invariance ESPRIT, IEEE Trans. on Sig. Proc., 40(4):867-881, April 1992.
[24] Song X, S. Zhou, P. Willett. Waveform Interference Mitigation for a Shared Spectrum MIMO Radar system. IEEE conf. on Radar, Pp 1386-1391, 2010
[25] Zheng Z., Jin Z and Zhang J. Joint DOD and DOA estimation of bistatic MIMO radar in the presence of unknown mutual coupling. Signal Processing 92 (2012) 3039–3048.
[26] Kundu D. Modified MUSIC algorithm for estimating DOA of signals, Signal Processing 48 (1996) 85 90.
[27] Capon J. High resolution frequency-wavenumber spectral analysis, Proc. IEEE, 57(8), 1408-1418, 1969.

AUTHOR'S PROFILE

First Author

David Ebregbe was born in 1963. Lecturer, Department of Electrical and Electronic Engineering, Niger Delta University, Wilberforce Island, Bayelsa State Nigeria. He holds a Bachelor of Engineering (B.Eng) degree from the University of Port harcourt , Nigeria – (1987). Master of Science (M.Sc) in Digital Communications system from Lough borough University. United Kingdom (2002). Doctor of Philosophy (Ph.D) in Communications and Information Engineering, Harbin Institute of technology, Harbin. China – (1913). Research interests include; Radar, Mobile and wireless Communication, Statistical and Array signal processing.